NANO LETTERS

Letter

pubs.acs.org/NanoLett

Electron Tunneling through Ultrathin Boron Nitride Crystalline Barriers

Liam Britnell,[†] Roman V. Gorbachev,[‡] Rashid Jalil,[‡] Branson D. Belle,[‡] Fred Schedin,[‡] Mikhail I. Katsnelson,[§] Laurence Eaves,[∥] Sergey V. Morozov,[⊥] Alexander S. Mayorov,[†] Nuno M. R. Peres,[#,▽] Antonio H. Castro Neto,[▽] Jon Leist,[◆] Andre K. Geim,[†,‡] Leonid A. Ponomarenko,[†] and Kostya S. Novoselov*[,†]

[†]School of Physics & Astronomy and [‡]Manchester Centre for Mesoscience & Nanotechnology, University of Manchester, Manchester M13 9PL, United Kingdom

[§]Institute for Molecules and Materials, Radboud University of Nijmegen, 6525 AJ Nijmegen, The Netherlands

[∥]School of Physics & Astronomy, University of Nottingham, Nottingham NG7 2RD, United Kingdom

[⊥]Institute for Microelectronics Technology, 142432 Chernogolovka, Russia

[#]Departamento de Física, Universidade do Minho, P-4710-057, Braga, Portugal

[▽]Graphene Research Centre and Department of Physics, National University of Singapore, 2 Science Drive 3, 117542, Singapore

[◆]Momentive Performance Materials, 22557 West Lunn Road, Strongsville, Ohio 4407

ABSTRACT: We investigate the electronic properties of ultrathin hexagonal boron nitride (h-BN) crystalline layers with different conducting materials (graphite, graphene, and gold) on either side of the barrier layer. The tunnel current depends exponentially on the number of h-BN atomic layers, down to a monolayer thickness. Conductive atomic force microscopy scans across h-BN terraces of different thickness reveal a high level of uniformity in the tunnel current. Our results demonstrate that atomically thin h-BN acts as a defect-free dielectric with a high breakdown field. It offers great potential for applications in tunnel devices and in field-effect transistors with a high carrier density in the conducting channel.

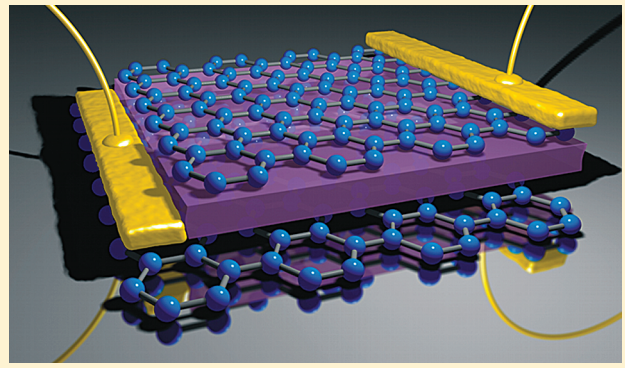

KEYWORDS: *Electron tunneling, boron nitride, graphene, ultrathin, conductive AFM*

Hexagonal boron nitride (h-BN) has great potential for use as the dielectric layer in functional heterostructure devices which exploit the remarkable properties of graphene.[1−4] The combination of graphene and h-BN opens up the exciting possibility of creating a new class of atomically thin multilayered heterostructures.[5,6] Graphene and h-BN share the same crystal structure and have very similar lattice constants, but unlike graphene, h-BN is an insulator with a large energy bandgap of 6 eV.[7,8] Previous studies have focused on the use of BN as a substrate for graphene electronics.[7,9,10] Thick boron nitride has also been used as a dielectric in experiments on coupled 2D electron gases,[11] as a barrier layer for electron tunnelling between two graphene layers[12] and in graphene vertical tunneling transistors.[13] Crystals of BN thicker than six layers are known to act as high-quality insulating layers when sandwiched between two graphene layers. Studying the performance of even thinner BN layers is of considerable fundamental interest and has the potential for new applications, such as devices for flexible electronics, especially as the layer thickness can, in principle, be controlled with atomic layer precision.

Here we investigate the electronic properties of tunnel diodes in which h-BN acts as a barrier layer between a variety of different conducting materials, such as graphene, graphite, and gold. We demonstrate that a single atomic layer of h-BN acts as an effective tunnel barrier and that the transmission probability of the h-BN barrier decreases exponentially with the number of atomic layers. The current−voltage characteristics of these devices show a linear $I-V$ dependence at low bias and an exponential dependence at higher applied voltages. We also used conductive atomic force microscopy (C-AFM) to measure the tunnel current through h-BN terraces of different thickness and found that the tunnel current on a particular terrace is spatially uniform and defect-free.

To investigate the electronic properties of the BN barriers, we fabricated several types of device, in the form of the following sandwich structures: Au/BN/Au, graphene/BN/graphene, and

Received: January 18, 2012
Revised: February 14, 2012
Published: March 1, 2012

graphite/BN/graphite. For the Au/BN/Au samples, we fabricated gold stripes of typical width, 2 μm, from a 5 nm Ti + 50 nm Au metallic bilayer deposited on a Si/SiO_2 substrate in which the oxide layer was 100 nm thick. Flakes of BN were then deposited on the metallic stripes using a micromechanical cleavage technique.[1] The flake thickness was characterized by a combination of optical contrast,[8] Raman spectroscopy, and AFM methods.[5] BN crystallites of different thicknesses that overlapped the gold contacts were identified,[8] and top contacts (5 nm Ti/50 nm Au) were deposited by electron beam or laser-writing lithography and electron gun evaporation.

We used an alternative technique to fabricate the graphene/BN/graphene and graphite/BN/graphite devices. To form the bottom electrode, micromechanical cleavage[1,5] was used to deposit narrow flakes of graphene (or graphite) on a SiO_2 substrate. Where necessary, the flakes were narrowed by reactive plasma etching through a poly(methyl methacrylate) mask. Similarly prepared and characterized BN crystals were deposited on the graphene (or graphite) flakes using a dry-transfer technique.[7,10] The top graphene (or graphite) electrode was transferred by the same method; (it could be shaped prior to transfer to achieve the desired overlapping area). Figure 1 shows representative images of our devices.

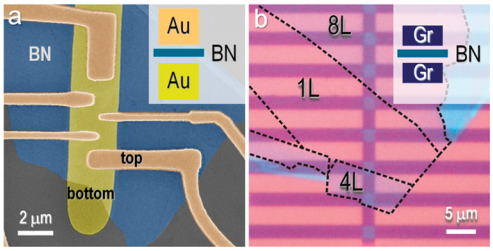

Figure 1. Micrographs of two of our devices. (A) A SEM micrograph of one of our Au/BN/Au devices (false colors). The bottom golden electrode is partly covered with six layers of BN (bluish area of irregular shape). Five top golden electrodes of different areas are then deposited on top of BN. Inset: schematic representation of the device. (B) An optical image of one of our graphite/BN/graphite devices. The bottom graphite layer is shaped by reactive plasma etching into several stripes of 2.5 μm width (horizontal purple lines). Thin BN layers have high transparency so the edges of BN crystallites with different numbers of layers are marked by black lines. Crossing of the top graphite layer (vertical purple line, 2.5 μm in width) forms several tunneling junctions with different thicknesses of BN. Inset: schematic representation of the device.

We measured the $I-V$ characteristics of our samples over a range of temperatures. The most reliable results were obtained with graphene or graphite as contact layers; for these devices, the measured current scaled accurately with the device area. However, with gold contacts, the data are somewhat less reproducible. We attribute this difference to the atomic flatness of the graphene and graphite layers. In contrast, the BN tunnel barrier may delaminate mechanically from the rough surface of the metallic layer, thus leading to a change in the active surface area of the device and to a reduction of the tunnel current. As shown in Figures 2 and 3, the $I-V$ curves of all our devices are linear around zero bias but have an exponential dependence on V at higher biases. The zero-bias conductivity for each type of device scales exponentially with the BN barrier thickness and is of the order of 1 $k\Omega^{-1}$ μm^{-2} for a monolayer BN sandwiched between gold and graphite electrodes, decreasing to approximately 0.1 $G\Omega^{-1}$ μm^{-2}

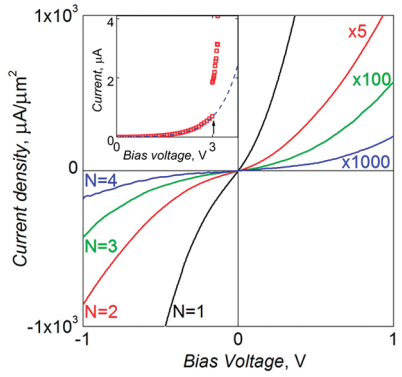

Figure 2. Characteristic $I-V$ curves for graphite/BN/graphite devices with different thicknesses of BN insulating layer: black curve, monolayer of BN; red, bilayer; green, triple layer; and blue, quadruple layer. Note the different scale for the four curves. Current was normalized by the realistic area of the tunneling barrier, which ranged 2−10 μm^2 depending on the particular device. The inset shows a typical $I-V$ curve where a breakdown in the BN is observed at +3 V, the thickness of the flake is 4 layers of BN (1.3 nm). The dotted line indicates the continuation of the exponential dependence.

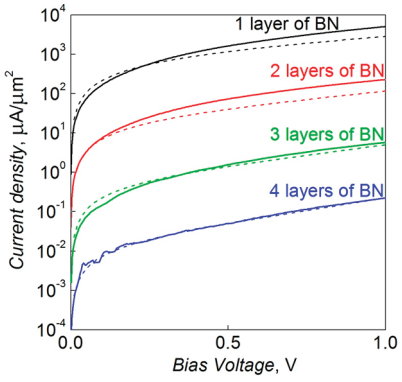

Figure 3. Same as Figure 2, just in log scale. Solid curves are experimental data, and dashed lines are our modeling. Only one fitting parameter for all four curves was used.

for devices with 4 BN atomic layers, see Figure 4. The Au/BN/Au and graphene/BN/graphene devices demonstrate similar behavior

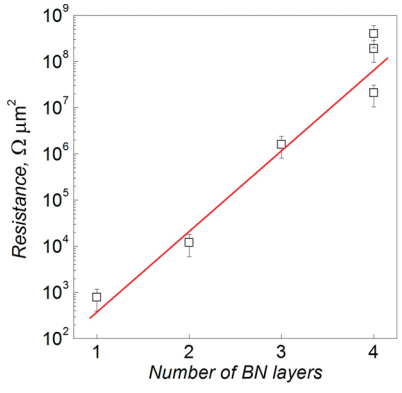

Figure 4. Exponential dependence of zero-bias resistance on the thickness of BN separating graphite and gold electrodes (1−4 layers of BN, 0.3−1.3 nm). Resistance is normalized to the area, which ranged 2−10 μm^2 depending on the particular device.

but with a larger spread of estimated current densities due to surface roughness and the effects of residual doping respectively.

dx.doi.org/10.1021/nl3002205 | Nano Lett. 2012, 12, 1707−1710

Figure 3 demonstrates the exponential dependence of the tunnel current on bias voltages above 0.5 V. Interestingly, for the graphene/BN/graphene and graphite/BN/graphite devices, this exponential dependence does not scale with barrier thickness. It is approximately independent of barrier thickness, which indicates that the tunnel current is dominated by the tunnelling density of states. Note, the situation for gold/BN/gold is different as the density of states in gold does not depend on the bias voltage, and so the growth of the conductance is determined solely by the reshaping of the barrier by the applied bias. For graphene and graphite electrodes, the behavior is more complicated but can be understood in terms of a simple theoretical model[14,15] in which the tunnel current is given by[15]

$$I(V) \propto \int \mathrm{d}E \mathrm{DoS}_{\mathrm{B}}(E)\mathrm{DoS}_{\mathrm{T}}(E - \mathrm{eV})T(E)[f(E - \mathrm{eV}) - f(E)]$$

where $f(E)$ is the Fermi distribution function, $\mathrm{DoS}_{\mathrm{T(B)}}(E)$ is the density of states in the top (bottom) electrode, and $T(E)$ is the transmission probability at the given energy. At low temperatures, the difference of the Fermi functions restricts the relevant energy E integral to $\mu < E < \mu + \mathrm{eV}$, where μ is the chemical potential. The above formula assumes that there is no in-plane momentum conservation, which is most likely to be the case of realistic graphene–hBN interfaces. There are several possible mechanisms for elastic scattering at the interface and, in particular, unavoidable fluctuations of the mass term due to the lattice mismatch. In our modeling we utilized a realistic density of states for graphene (graphite) and assumed the hole tunneling with effective mass $m = 0.5m_0$ (m_0 is the free electron mass) and the height of the tunneling barrier $\Delta \approx 1.5$ eV.[16,17]

In order to examine the uniformity and defect density in the BN insulating barrier layer, we carried out a separate set of experiments using an AFM tip as the top electrode and graphite as the lower electrode, see Figure 3. When the AFM tip was maintained at the same position (with negligible thermal drift), the $I-V$ characteristics were very similar to those obtained for the graphite/BN/graphite samples. By comparing the tunnel currents obtained on the graphite/BN/graphite and the graphite/BN/tip devices, we were able to estimate the active area of the tip to be $\sim 10^3$ nm^2, in reasonable agreement with the number expected for metal-coated AFM tips with nominal radius of 10 nm. For the AFM tip experiments, we observed little variation in the amplitude of the current for repeated ramps in bias voltage. This suggests that the effective area of the contact varied little over the course of the experiment. However, one would anticipate that the tip area could change due to the mechanical forces exerted by the sample surface.[18] To this end, we made sure that the elastic forces exceeded the Coulomb attraction at all times, which guarantees constant area of the contact even at high applied biases. Several similar tips were used on a range of samples: The resulting $I-V$ curves followed the same trend for all tip and sample combinations, with only small discrepancies in current due to differing tip shapes/areas.

We also scanned graphite/BN sandwich devices with conducting AFM tips in contact mode with a constant bias applied between the graphite layer and tip (Figure 5). The resistance map is very uniform, with only small variations of about 10%. For nearly all of the devices, we observed no evidence of pinholes or defects, even though areas of tens of square micrometers were scanned. We have also tested the uniformity of the breakdown voltage by measuring it at more than 20 different spots on mono- as well as several layers of

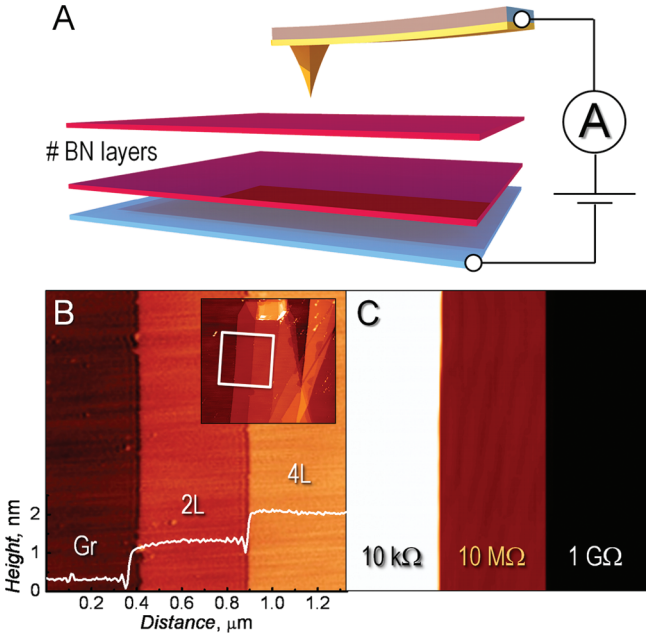

Figure 5. Local mapping of the tunneling current through BN terraces over micrometer scale regions by C-AFM measurements. (A) Schematic representation of the setup. Graphite (the blue plane) is covered by several layers of BN. A conductive AFM probe is used to scan the surface, and the tunneling current recorded as a function of the tip position. (B) Topography measured by tapping-mode AFM. The inset shows the overall region and the height profile shows that BN has a low roughness (<1 nm rms). (C) The leakage current measured at the same position as topography in (B). There is little variation of leakage current on regions of the same thickness, suggesting a lack of pin holes or other defects that would lead to spikes in the measured current.

hBN (see Figure 2). Typical breakdown fields we obtained were of the order of 1 GV m^{-1}, which is in agreement with that measured in other thin BN samples.[18] This demonstrates that BN can be used as an atomically thin, high-quality insulator.

In conclusion, we have demonstrated a method for fabricating devices with atomically thin tunnel barriers by cleaving few layer flakes from an h-BN crystal and transferring them without contamination to a suitable contact electrode layer, namely graphene, graphite, or Au mounted on a Si/SiO_2 substrate. A variety of devices can be fabricated by using different combinations of these materials for the upper and lower electrodes. Our measurements of the electron tunnel current through the barrier demonstrate that the BN films act as a good tunnel barrier down to a single atomic plane. Current–voltage measurements were made for different BN thicknesses, from one to four atomic layers. The $I-V$ curves are linear at low bias but take on an exponential dependence at higher bias (>0.5 V). The tunnel current is exponentially dependent on the BN barrier thickness, as expected for quantum tunneling. Our C-AFM measurements indicate that the tunnel current is uniform when the tip is scanned across micrometer scale areas of a flat BN atomic layer, indicating an absence of pinholes and defects in the BN crystal. We conclude that h-BN is a high quality, ultrathin, low dielectric constant barrier material, which has great potential for use in novel electron tunneling devices and for investigating strongly coupled and narrowly separated electrodes of different compositions (graphene, graphite, or metal). Of particular interest is the possibility of studying the electronic properties of

dx.doi.org/10.1021/nl3002205 | Nano Lett. 2012, 12, 1707–1710

two closely spaced graphene layers separated by a BN barrier of one or more atomic layer thicknesses.

AUTHOR INFORMATION

Corresponding Author

*Email: kostya@manchester.ac.uk. Telephone: +44-(0)161-275-41-19.

Notes

The authors declare no competing financial interest.

ACKNOWLEDGMENTS

This research was supported by the European Research Council, European Commision FP7, Engineering and Physical Research Council (U.K.), the Royal Society, U.S. Office of Naval Research, U.S. Air Force Office of Scientific Research, and the Körber Foundation. A.H.C.N. acknowledges the NRF-CRP award "Novel 2D materials with tailored properties: beyond graphene" (R-144-000-295-281).

REFERENCES

(1) Novoselov, K. S.; Geim, A. K.; Morozov, S. V.; Jiang, D.; Zhang, Y.; Dubonos, S. V.; Grigorieva, I. V.; Firsov, A. A. Electric field effect in atomically thin carbon films. *Science* **2004**, *306* (5696), 666−669.

(2) Geim, A. K.; Novoselov, K. S. The rise of graphene. *Nat. Mater.* **2007**, *6* (3), 183−191.

(3) Geim, A. K. Graphene: status and prospects. *Science* **2009**, *324* (5934), 1530−1534.

(4) Castro Neto, A. H.; Guinea, F.; Peres, N. M. R.; Novoselov, K. S.; Geim, A. K. The electronic properties of graphene. *Rev. Mod. Phys.* **2009**, *81* (1), 109−162.

(5) Novoselov, K. S.; Jiang, D.; Schedin, F.; Booth, T. J.; Khotkevich, V. V.; Morozov, S. V.; Geim, A. K. Two-dimensional atomic crystals. *Proc. Natl. Acad. Sci. U.S.A.* **2005**, *102* (30), 10451−10453.

(6) Novoselov, K. S. Nobel Lecture: Graphene: Materials in the Flatland. *Rev. Mod. Phys.* **2011**, *83* (3), 837−849.

(7) Dean, C. R.; Young, A. F.; Meric, I.; Lee, C.; Wang, L.; Sorgenfrei, S.; Watanabe, K.; Taniguchi, T.; Kim, P.; Shepard, K. L.; Hone, J. Boron nitride substrates for high-quality graphene electronics. *Nat. Nanotechnol.* **2010**, *7* (9), 693−696.

(8) Gorbachev, R. V.; Riaz, I.; Nair, R. R.; Jalil, R.; Britnell, L.; Belle, B. D.; Hill, E. W.; Novoselov, K. S.; Watanabe, K.; Taniguchi, T.; Geim, A. K.; Blake, P. Hunting for monolayer boron nitride: optical and Raman signatures. *Small* **2011**, *7* (4), 465−468.

(9) Ponomarenko, L. A.; Yang, R.; Mohiuddin, T. M.; Katsnelson, M. I.; Novoselov, K. S.; Morozov, S. V.; Zhukov, A. A.; Schedin, F.; Hill, E. W.; Geim, A. K. Effect of a high-κ environment on charge carrier mobility in graphene. *Phys. Rev. Lett.* **2009**, *102* (20), 206603.

(10) Mayorov, A. S.; Gorbachev, R. V.; Morozov, S. V.; Britnell, L.; Jalil, R.; Ponomarenko, L. A.; Blake, P.; Novoselov, K. S.; Watanabe, K.; Taniguchi, T.; Geim, A. K. Micrometer-Scale Ballistic Transport in Encapsulated Graphene at Room Temperature. *Nano Lett.* **2011**, *11* (6), 2396−2399.

(11) Ponomarenko, L. A.; Geim, A. K.; Zhukov, A. A.; Jalil, R.; Morozov, S. V.; Novoselov, K. S.; Grigorieva, I. V.; Hill, E. H.; Cheianov, V. V.; Fal'ko, V. I.; Watanabe, K.; Taniguchi, T.; Gorbachev, R. V. Tunable metal−insulator transition in double-layer graphene heterostructures. *Nat. Phys.* **2011**, *7* (12), 958−961.

(12) Amet, F.; Williams, J. R.; Garcia, A. G. F.; Yankowitz, M.; Watanabe, K.; Taniguchi, T.; Goldhaber-Gordon, D. Tunneling spectroscopy of graphene-boron nitride heterostructures. *Phys. Rev. B* **2012**, *85* (7), 073405.

(13) Britnell, L.; Gorbachev, R. V.; Jalil, R.; Belle, B. D.; Schedin, F.; Mishchenko, A.; Georgiou, T.; Katsnelson, M. I.; Eaves, L.; Morozov, S. V.; Peres, N. M. R.; Leist, J.; Geim, A. K.; Novoselov, K. S.; Ponomaremko, L. A. Field-Effect Tunneling Transistor Based on Vertical Graphene Heterostructures. *Science* **2012**, *335*, 947−950.

(14) Simmons, J. G. Generalized formula for the electric tunnel effect between similar electrodes separated by a thin insulating film. *J. Appl. Phys.* **1963**, *34* (6), 1793−1803.

(15) Wolf, E. L. *Principles of electron tunneling spectroscopy*; Oxford University Press: Oxford, U.K., 1985.

(16) Kharche, N.; Nayak, S. K. Quasiparticle band gap engineering of graphene and graphone on hexagonal boron nitride substrate. *Nano Lett.* **2011**, *11* (12), 5274−5278.

(17) Xu, Y. N.; Ching, W. Y. Calculation of ground-state and optical properties of boron nitrides in the hexagonal, cubic, and wurtzite structures. *Phys. Rev. B* **1991**, *44* (15), 7787−7798.

(18) Lee, G.-H.; Yu, Y.-J.; Lee, C; Dean, C; Shepard, K. L.; Kim, P.; Hone, J. Electron tunneling through atomically flat and ultrathin hexagonal boron nitride. *Appl. Phys. Lett.* **2011**, *99*, 243114.